# Quantum Dot Sensitization of Organic−Inorganic Hybrid Solar Cells

**Robert Plass,* Serge Pelet, Jessica Krueger, and Michael Grätzel**

*Institute of Molecular and Biological Chemistry, School of Basic Sciences, Swiss Federal Institute of Technology, 1015 Lausanne, Switzerland*

**Udo Bach**

*NTera Ltd., c/o G.S.K. Grangeroad, Rathfarnham, Dublin 16, Ireland*

*Received: February 19, 2002; In Final Form: May 29, 2002*

A high surface area pn-heterojunction between $TiO_2$ and an organic p-type charge transport material (spiro-OMeTAD) was sensitized to visible light using lead sulfide (PbS) quantum dots. PbS quantum dots were formed in situ on a nanocrystalline $TiO_2$ electrode using chemical bath deposition techniques.[1] The organic hole conductor was applied from solution to form the sensitized heterojunction. The structure of the quantum dots was analyzed using HRTEM technique. Ultrafast laser photolysis experiments suggested the initial charge separation to proceed in the subpicosecond time range. Transient absorption laser spectroscopy revealed that interfacial charge recombination of the initially formed charge carriers is much faster than in comparable dye-sensitized systems.[2,3] The sensitized heterojunction showed incident photon-to-electron conversion efficiencies (IPCE) of up to 45% and energy conversion efficiencies under simulated sunlight AM1.5 (10 mW/cm2) of 0.49%.

## Introduction

Quantum dots are very interesting as a sensitizer for wide band gap semiconductor materials.[4] IPCE values in PbS sensitized photoelectrochemical cells (PEC) reach nearly 80% with good light harvesting properties up to 800 nm.[1] Unfortunately, quantum dot sensitized PEC solar cells generally suffer severe photostability problems. Novel inorganic−organic hybrid photovoltaic systems,[3,5] however, might offer much more suitable conditions for the application of inorganic semiconductor quantum dots as optical sensitizers. Corrosion and photocorrosion effects generally observed in PEC cells are mainly due to the aggressive nature of the electrolyte employed and mass transport phenomena, which lead to photoinduced particle growth. Photocorrosion generally involves chemical reactions of charge carriers with the electrolyte or the bulk material itself. Fast charge transfer from the quantum dot to the neighboring p- and n-type materials will therefore be crucial to suppress photocorrosion phenomena. Solid-state organic−inorganic heterojunction systems might provide the desired environment for quantum dot sensitization, as there is no charge transfer involved in the regeneration process, which can occur very rapidly.

The photovoltaic performance of the quantum dot sensitized heterojunction was studied by means of sandwich type cells. The PbS quantum dots were synthesized in situ onto the mesoporous $TiO_2$ substrate using a chemical bath deposition technique.[1,6,7]

## Experimental Section

The working electrode consists of conducting glass (fluorine-doped $SnO_2$, sheet resistance 10 Ohms/square) onto which a compact $TiO_2$ layer was deposited by spray pyrolysis.[8] This avoids direct contact between the organic charge transport material and the doped $SnO_2$ layer, which would short-circuit the cell. A 2.5 $\mu$m thick mesoporous film of $TiO_2$ was deposited by screen-printing onto the compact layer.

The mesoporous electrodes were dipped for 1 min into an aqueous saturated lead nitrate solution, rinsed meticulously with water, and then dipped into a 0.2 M $Na_2S$ solution and rinsed again with water (this will be referred to as one full coating cycle). Different particles size could be obtained by repeating the coating procedure several times.

The organic charge transport material was introduced into the mesopores by spin coating a 0.17 M chlorobenzene solution of spiro-OMeTAD onto the $TiO_2$ film and subsequently evaporating the solvent. The spin-coated solution contained two additives. One, $N(p\text{-}C_6H_4Br)_3SbCl_6$ (0.38 mM), was used for partial oxidation of spiro-OMeTAD controlling the doping level.[5] As second additive, $Li[CF_3SO_2]_2N$ (0.2 mM), was added since lithium ions have been shown to increase the current output and the overall efficiency of the solid-state device (SSD).[5] Finally a semitransparent gold back contact was evaporated on top of the hole conductor under vacuum.

Transmission electron microscopy was performed using a Philips CM300. Absorption spectra were measured on a Cary 5 UV/Vis/NIR spectrophotometer. The fluorescence was taken on a SPEX fluorolog 112 and excited with a Coherent Innova Kr laser at 468 nm. IPCEs were measured with a 400 W Xe lamp. For current−voltage characteristics, we used a sulfur lamp as light source. Flash photolysis experiments were carried out with a Nd:YAG laser as excitation source, providing 6 ns pulses at a repetition rate of 30 Hz. The triplet of the laser fundamental (355 nm) was sent into an OPO used to tune the pump wavelength. The probe light intensity from a Xe lamp was measured by a fast photomultiplier after passing through a monochromator. The data were averaged over 2000 laser shots by a 1 GHz band-pass digital oscilloscope. A more detailed description of the femtosecond spectrometer will be published

* Corresponding author. E-mail: robert.plass@epfl.ch

10.1021/jp020453l CCC: $22.00 
Published on Web 07/16/2002


**Figure 1.** HRTEM picture of a $TiO_2$ nanocrystal (15 nm) sensitized with PbS nanoparticles (6 nm).

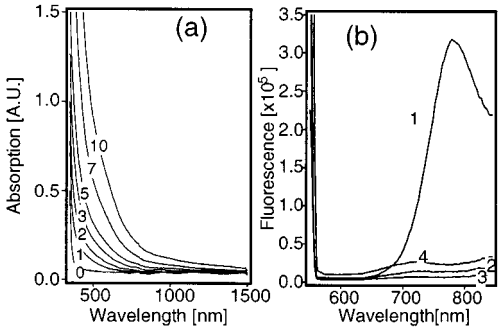


**Figure 2.** Total diffuse transmission and fluorescence spectra: (a) the diffuse transmission spectra of 2 $\mu$m $TiO_2$ layer after various number of coatings with PbS. (b) Fluorescence spectra: comparison between different semiconductor 2 $\mu$m thick layers ($ZrO_2$ and $TiO_2$). (1) $ZrO_2$ + PbS, (2) $ZrO_2$, (3) $TiO_2$ + PbS, (4) $TiO_2$. All PbS sensitized samples were prepared with five coating cycles.

elsewhere.[9] Briefly, the ultrafast dynamics measurements were carried using the pump−probe technique. The fundamental of the femtosecond laser source (CPA 2001 from Clark-MXR) was used to probe the sample at 778 nm, while the pump beam at 600 nm and the probe beam at 1400 nm were generated by two noncollinear OPAs. After the interaction with the pump pulse in a moving sample, the probe beam intensity was measured by a diode. The diode signal was analyzed by a lock-in amplifier tuned at the frequency of a chopper placed on the pump pathway.

## Results and Discussion

Figure 1 shows an HRTEM picture of $TiO_2$ coated with PbS nanoparticles. The $TiO_2$ crystal onto which the PbS crystals have grown is clearly visible. On this sample, the average size of the particles obtained after seven coatings is 6 nm. The structure of PbS crystals is cubic galena.[6] The two semiconductors have been discriminated through diffraction pattern analysis.

Figure 2a shows the transmission spectra of a mesoporous $TiO_2$ film after several consecutive deposition steps. A strong increase in absorption after each step can be observed, suggesting an increase in the number of particles as well as a bathochromic spectral shift. This effect can be explained by an increase in the size after each deposition step in terms of the size quantization effect.

Fluorescence spectroscopy was also carried out on these films; the results are shown in Figure 2b. The samples were excited with a Krypton laser at 520 nm. The aim of these measurements was to compare the behavior of PbS placed on different substrates, i.e., $TiO_2$ and $ZrO_2$. In the case of $TiO_2$, the fluorescence is totally quenched due to the injection of the electron into the semiconductor. The higher lying conduction band of $ZrO_2$ prevents this reaction from occurring; therefore, the PbS luminescence is observed when this insulator is used as a support. The minor differences in the signal intensities of the nonfluorescing samples can be attributed to measurements errors, since they depend strongly on the angle of the sample toward the excitation light, which is difficult to maintain constant.

Femtosecond and nanosecond laser experiments were carried out to study the dynamics occurring in the system after excitation:

$$\mathrm{PbS} \xrightarrow{h\nu} \mathrm{h^+(PbS) + e^-(PbS)}$$

$$\mathrm{e^-_{free}(PbS) \rightarrow e^-_{trap}(PbS)} \quad (1)$$

$$\mathrm{e^-_{trap}(PbS) \rightarrow e^-_{cb}\,(TiO_2)} \quad (2)$$

$$\mathrm{e^-(PbS) + h^+(PbS) \rightarrow \Delta} \quad (3)$$

$$\mathrm{h^+(PbS) + spiro\text{-}OMeTAD \rightarrow h^+(spiro\text{-}OMeTAD)} \quad (4)$$

$$\mathrm{e^-(TiO_2) + h^+(spiro\text{-}OMeTAD) \rightarrow \Delta} \quad (5)$$

The very fast processes (eqs 1 2, 3, 4) are illustrated in Figure 3a. Measurements were done on PbS sensitized semiconductor layers deposited on glass. These samples can be seen as open circuit cells. The samples were excited at 600 nm with the femtosecond laser. At this wavelength the PbS nanoparticles still absorb a large amount of light. A probe pulse centered around 778 nm was used to monitor the different reactions occurring inside the PbS. The measurements were done for PbS sensitized $TiO_2$ and $ZrO_2$; the results are shown in the inset of Figure 3a. The data were best fitted by a double exponential decay. For both semiconductors the first component is identical, having a time constant around 1ps, and can be attributed to the electron trapping (eq 1). The slower decay differs from one oxide support to the other. For $TiO_2$, the time constant is smaller (20 ps) compared to $ZrO_2$ (30 ps). On $TiO_2$, the trapped electron is injected into the conduction band (eq 2). On the contrary, on $ZrO_2$ the electron−hole pair recombine (eq 3). These results are in good agreement with previous measurements.[10] Another probe wavelength of 1400 nm was chosen (Figure 3a), to monitor the electrons in the $TiO_2$ and the oxidized hole conductor. The absorption spectra of the spiro-OMeTAD shown in Figure 3c was taken from the literature.[11] At 1400 nm, the trapping kinetics are very similar to those measured at 778 nm, the measured time constant is 1.1ps. In the case of $TiO_2$, the second time constant is slower (80 ps) than at 778 nm. This difference can be explained by the fact that electrons in the $TiO_2$ conduction band absorb at this wavelength and have a longer lifetime than those in the PbS. In the case of $ZrO_2$, only the trapping dynamics can be observed and no longer lasting contribution to the signal was measured. As the maximum intensity of the signal for $ZrO_2$ is small, the signal from the

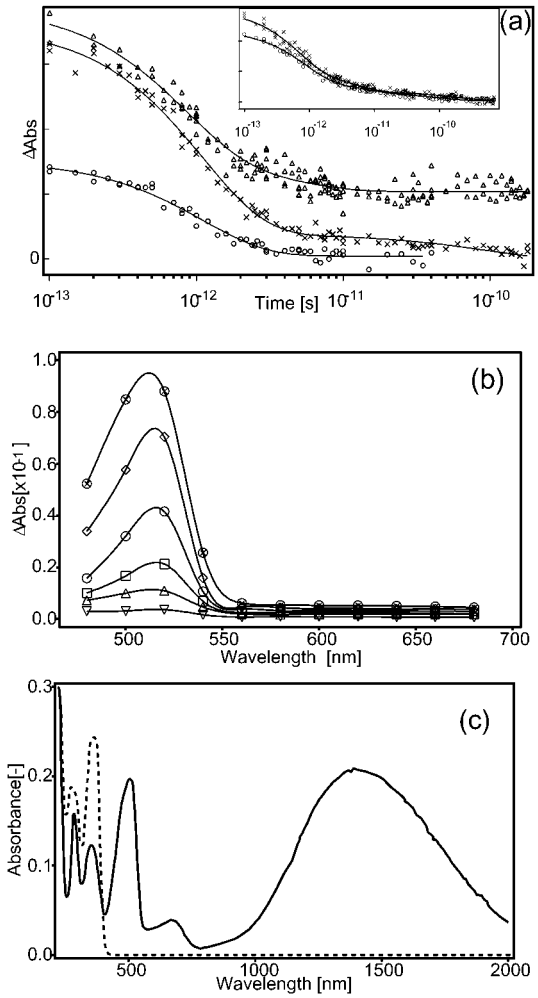


**Figure 3.** (a) Transient absorption kinetics of a 2 $\mu$m $ZrO_2$ layer sensitized with PbS (○), a 2.5 $\mu$m $TiO_2$ layer sensitized with PbS (×), and a 2.5 $\mu$m $TiO_2$ sensitized with PbS and spin-coated with hole conductor solution (△). The excitation light wavelength was 600 nm and the probe light wavelength 1400 nm (778 nm in the case of the inset). (b) Transient absorption difference spectra, excitation wavelength 450 nm, of a 3 $\mu$m $TiO_2$ layer sensitized by PbS (coated five times) and spin-coated with hole conductor solution at different time delays: ⊗, $5 \times 10^{-7}$s; ◇, $10^{-6}$s; ○, $2 \times 10^{-6}$ s; □, $4 \times 10^{-6}$ s; △, $8 \times 10^{-6}$ s; ▽, $6 \times 10^{-5}$ s. (c) Absorption spectra of OMeTAD (dashed line) and $OMeTAD^{2+}$ (solid line) in $CH_2Cl_2$.

trapped electrons may be buried in the background noise. Therefore, it cannot be excluded that the trapped electrons in PbS also contribute to the longer lasting signal measured with $TiO_2$ at this wavelength.

When the $TiO_2$ device is completed with the hole conductor, the oxidation of this species can be observed. This reaction is due to the transfer of a hole from a PbS particle to a spiro-OMeTAD molecule (eq 4). In this case, the decay is also fitted to a double exponential. The fit produced two time constants. The first, around 1 ps, is typical for electron trapping in PbS. The second, 4 ps, is the representation of the transfer of the hole into the spiro-OMeTAD (eq 4).

The recombination of an electron in the $TiO_2$ and a hole in the spiro-OMeTAD (eq 5) was measured with a nanosecond laser and can be seen in Figure 3b. The sample was excited at 450 nm and the spectral changes recorded in the 480 to 680 nm wavelength region. The absorption peak at 518 nm is characteristic for the oxidized state of the spiro-OMeTAD. It is decreasing with time; showing the recombination (eq 5). The

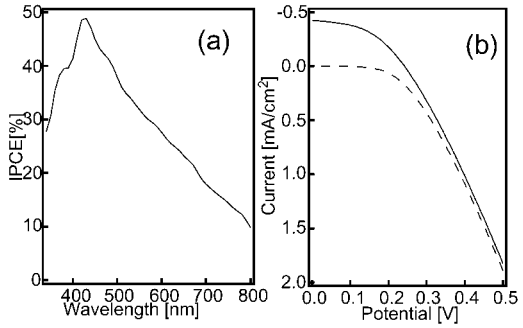


**Figure 4.** (a) IPCE of a PbS solid-state sensitized solar cell. The hole conductor matrix was 0.2 mM in $Li(CF_3SO_2)_2N$ and 0.38 mM in $N(p\text{-}C_6H_4Br)_3SbCl_6$. (b) Current−voltage characteristics in the dark (dashed line) and at an illumination intensity of 1/10 sun (corresponding to global AM1.5 10 mW/cm$^2$).

recombination time constant has been measured to be 2 $\mu$s. The presence of oxidized spiro-OMeTAD is a proof for the regeneration of PbS by the hole conductor.

By measuring devices with different number of coatings, it can be seen that an optimum for performance of the cell exists. Figure 4a shows an IPCE measurement for what turned out to be the optimum, i.e., five coatings for a $TiO_2$ thickness of 2.5 $\mu$m. It can also be seen that the maximum is 45% and lies at around 420 nm. It is remarkable that at 800 nm there is still a significant signal. The size optimum is determined by a tradeoff between visible light harvesting and PbS conduction band position; i.e., electron injection. These two phenomena are related to the quantum size effect. The hole-conductor matrix was 0.2 mM in $Li(CF_3SO_2)_2N$ and 0.38 mM in $N(p\text{-}C_6H_4\text{-}Br)_3SbCl_6$.

Figure 4b shows *I*/*V* characteristics of a typical cell sensitized by PbS at illumination of 10% sun (10 mW/cm$^2$). The open circuit potential ($U_{OC}$) is 240 mV and the overall efficiency 0.49%.

In conclusion, quantum-dot sensitized solid-state solar cells based on spiro-OMeTAD have been shown to be an interesting alternative to the dye sensitized systems. Further work is in progress to improve the efficiency of these cells.

**Acknowledgment.** We thank Dr. Spreitzer (Covion) for supplying us with spiro-OMeTAD. We also thank Prof. Stadelmann (CIME/EPFL) for performing the HRTEM experiments and for his help in the interpretation of the results. Further, we acknowledge support from the Swiss National Science Foundation.

## References and Notes

(1) Vogel, R.; Hoyer, P.; Weller, H. *J. Phys. Chem.* **1994**, *98*, 3183.
(2) Bach, U.; Tachibana, Y.; Moser, J.-E.; Haque, S. A.; Klug, D. R.; Grätzel, M.; Durrant, J. R. *J. Am. Chem. Soc.* **1999**, *121*, 7445.
(3) Krueger, J.; Bach, U.; Plass, R.; Cevey, L.; Piccirelli, M.; Grätzel, M. *Appl. Phys. Lett.* **2001**, *79*, 2085.
(4) Zaban, A.; Micic, O. I.; Gregg, B. A.; Nozik, A. J. *Langmuir* **1998**, *14*, 3153.
(5) Bach, U.; Lupo, D.; Comte, P.; Moser, J. E.; Weissörtel, F.; Salbeck, J.; Spreitzer, H.; Grätzel, M. *Nature* **1998**, *395*, 583.
(6) Weller, H.; Eychmüller, A.; Vogel, R.; Katsikas, L.; Hässelbarth, A.; Giersig, M. *Isr. J. Chem.* **1993**, *33*, 107.
(7) Weller, H. *Adv. Mater.* **1993**, *5*.
(8) Kavan, L.; Grätzel, M. *Electrochim. Acta* **1995**, *40*, 643.
(9) Pelet, S.; Moser, J.-E.; Grätzel, M., to be published.
(10) Patel, A. A.; Wu, F.; Zhang, J. Z.; Torres-Martinez, C. L.; Mehra, R. K.; Yang, Y.; Risbud, S. H. *J. Phys. Chem. B* **2000**, *104*, 11598.
(11) Weissörtel, F. Amorphe niedermolekulare Ladungstransportmaterialien für nanokristalline Solarzellen. Diplomarbeit, Universität Regensburg, 1996.